A New Passive Lossless Snubber

Erlan Dzhunusbekov and Sagi Orazbayev

***Abstract*—Galvanically isolated photovoltaic (PV) microinverters based on single-stage flyback topology have advantages: simplicity, better reliability, and low cost. But isolated flyback topology comes with voltage stresses on semiconductor switches caused by transformer leakage inductance. An improved regenerative snubber has been proposed to meet the ever-growing demand for higher efficiency of PV microinverters. The proposed topology is the inductor-capacitor-diode (LCD) snubber with flying capacitor modified to reduce circulating currents. Theoretical analysis reveals a number of advantages. Experimental results are presented to verify the performance.**

***Index Terms*—Flyback, LCD snubber, PV microinverter, regenerative flying capacitor snubber.**

I. Introduction

MICROINVERTERS convert power at the module level utilizing more solar energy from an individual photovoltaic (PV) panel and removing the risk of a single point failure. Therefore, microinverters have gained fame for energy harvest increase and reliability improvement. Since they are contributing to the growth of distributed solar worldwide, there is a high demand for more efficient and low-cost microinverters. The improvements in power semiconductors and magnetic components make flyback topology more efficient and attractive in various low power applications. Flyback topology has a low component count, simple schematics, excellent robustness, and a possibility to provide galvanic isolation; thus, it would be a good idea to keep up with flyback topology for PV microinverters with galvanic isolation. But one of the major challenges encountered here by designers is the voltage stresses mitigation of semiconductor switches caused by flyback transformer leakage inductance. For better efficiency, those voltage stresses have to be suppressed by implementing a nondissipative clamp preferably the most efficient and passive one to maintain low cost.

Manuscript received September 4, 2020; revised December 3, 2020; accepted January 15, 2021. Date of publication February 2, 2021; date of current version May 5, 2021. This work was supported by the Science Committee of the Ministry of Education and Science of the Republic of Kazakhstan in the framework of the project "Research and development of an innovative micro-inverter for photovoltaic panels" under Project AP 05135334. Recommended for publication by Associate Editor G. Moschopoulos. *(Corresponding author: Erlan Dzhunusbekov.)*

Erlan Dzhunusbekov is with the Laboratory of Advanced Developments in Electronics, Kazakh-British Technical University, Almaty 050010, Kazakhstan (e-mail: erlan555dj@yahoo.com).

Sagi Orazbayev is with the National Nanotechnology Lab, Al-Farabi Kazakh National University, Almaty 050040, Kazakhstan (e-mail: sagi.orazbayev@gmail.com).

Color versions of one or more figures in this article are available at https://doi.org/10.1109/TPEL.2021.3056189.

Digital Object Identifier 10.1109/TPEL.2021.3056189

There are several solutions proposed to limit voltage spikes on the main switch with the leakage energy recovery of a flyback transformer.

Active clamp snubbers with regenerative capabilities [1]–[5] can help effectively recover the transformer leakage energy, also helping to provide zero voltage switching (ZVS) for the main power transistor [3]–[5]. But, all of these benefits come with the complexity of the active clamp. Also, the active clamp reduces the robustness of a flyback topology. First, there is the possibility of destructive shoot-through currents between the conducting clamp switch and the main transistor configured as the half-bridge circuit. Second, the topology is vulnerable for output short circuit commutations because the auxiliary clamp switch commutates the snubber capacitor to the output capacitor through the transformer leakage inductance of a small value.

There are also some snubbers [6]–[8] with the straight forward idea of the commutation of clamp capacitor to input to recover transformer leakage energy. For example, in [6], a flyback converter is claimed with the additional auxiliary dc/dc converter that recovers leakage energy temporally stored in a snubber capacitor back to the input. This is a costly solution not efficient for low power applications but effective and justified in high power converters. For example, in a PV microinverter flyback with the peak power up to 300 W, the transformer leakage energy loss rate could reach 10 W, which might be worth recycling with an additional converter. In [7] and [8], the snubber embodies a semiactive auxiliary switch that commutates the clamp capacitor to the input through the auxiliary inductor synchronously with the flyback main switch. These mentioned snubbers [6]–[8] are featured with the complex structure but do not have a risk of shoot-through current or a clamp capacitor short-circuited to the output.

There are also a number of passive nondissipative snubber circuits for flyback converter [9]–[13] known as inductor-capacitor-diode (LCD) snubbers, the general circuit is in Fig. 1.

It is reported that these passive snubbers reduce turn-OFF switching losses and effectively regenerate leakage energy. The auxiliary flying capacitor C_{x} in Fig. 1 resonantly recharges to peak voltages of opposite polarities; therefore, there are additional circulating currents in snubber circuits that cause extra power dissipation in snubber components. Before the main transformer discharges to the secondary side, the snubber recovers leakage energy back to an input power supply at the beginning of the main transistor $\mathrm{Q_m}$ turn-OFF stage, delaying the conduction of the flyback secondary side [14]. This delay eats out fractions from conduction cycles of primary and secondary sides; thus, increasing rms in the flyback circuit. There are versions of regenerative circuits [15], [16], where snubber inductor L_{x} in

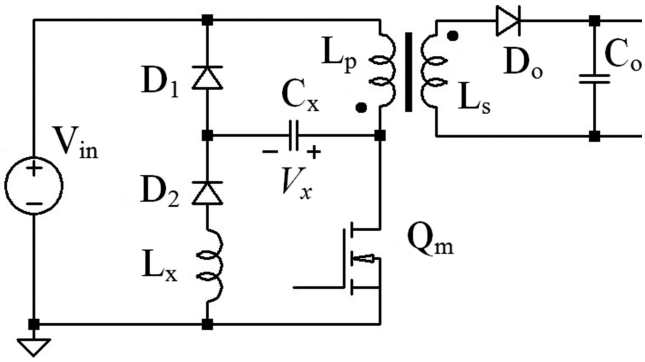

Fig. 1. Flyback converter with conventional lossless LCD snubber.

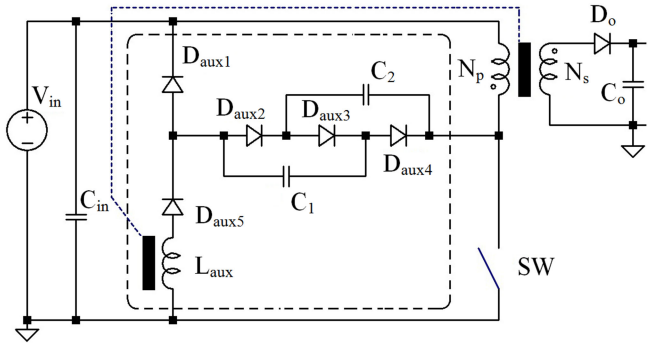

Fig. 2. Flyback converter with the proposed lossless LCD snubber.

Fig. 1 is integrated on the same magnetic core as the main transformer. This offers the advantage of reducing component count. Another advantage of the passive integrated regenerative snubber is that it recovers part of transformer leakage energy back to the magnetizing inductor of a flyback main transformer. Thus, it releases part of a captured leakage energy before the main transistor Q_m turn-OFF. As a consequence, the integrated snubber has reduced current rms in snubber circuits. Another consequence is that it takes less time to discharge the remaining portion of leakage energy; therefore, current on the secondary side ramps up faster. It is reported [16] that the integrated LCD snubber demonstrates higher efficiency than the nonintegrated version. In integrated and nonintegrated LCD snubbers, the bigger the value of a capacitor C_{x}, the lesser the voltage spike would be on the main transistor $\mathrm{Q_m}$. Controlling the voltage spike comes at the expense of higher values of circulating currents in the snubber and higher rms in a flyback.

The authors in [14] proposed to add a capacitor-diode (CD) snubber circuit on the flyback secondary side to mitigate the adverse influence of the resonant LCD snubber on the flyback rms. The additional snubber receives energy from the primary side power supply at the beginning of the turn-ON stage and releases it to the output at the beginning of the turn-OFF stage. This results in secondary current ramping up faster. The circulating currents in the combined primary LCD and secondary CD snubber do not reduce but redistribute between snubbers depending on the ratio of snubber capacitors' values.

The authors in [17] proposed to implement a complex auxiliary transformer to passively switch over the leakage energy captured by the clamp capacitors from the primary side to the secondary side. The auxiliary transformer would require meeting isolation standards. The recovery process using a transformer might not be efficient.

Most of the problems of the above mentioned regenerative LCD snubber and its variations are side effects of the resonant mode of their operation. The resonant mode helps to reach ZVS and zero current switch (ZCS) for the main flyback switch. But for low voltage applications, such as in our particular case, a microinverter for photovoltaic panels, the switching losses of the main primary switch are not predominant. In Section III, it is shown that the traditional snubber will perform better with the constant voltage of the snubber capacitor although the primary switch is hard switching. But, there is a limit for the conventional LCD snubber to operate in this way. The voltage of the snubber capacitor must be big enough to reverse the flyback transformer at a reasonable time for better efficiency. That is not always possible. Therefore, a modification for the conventional LCD snubber was proposed [18] (see Fig. 2) and its advantages are proved in this article.

As seen in Fig. 2 the considered snubber is a modified LCD flying capacitor snubber designed to have increased clamping voltage V_c as the sum of capacitors C_1 and C_2 voltages that leads to an implementation expansion. The L_{aux} inductor can be a separate inductor or integrated with the main flyback transformer. The integrated version of the proposed snubber may be designed in such a way that during primary switch SW conduction the snubber capacitors would be applied to the auxiliary transformer winding L_{aux} charging the transformer. In this article, only a nonintegrated version of a new snubber is considered.

The rest of this article is organized as follows. In Section II, the proposed snubber is introduced. In Section III, the advantages of the nonresonant operation mode of proposed and conventional LCD snubbers are discussed. In Section IV, it is shown how the conventional snubber affects flyback rms, and how the proposed snubber improves efficiency. Experimental proofs and thorough quantitative power loss analysis are provided. Finally, Section V concludes the article.

II. Proposed Regenerative Snubber Circuit

In Fig. 2, one can see the voltage limiter consisting of clamp capacitors C_1 and C_2, clamp diodes D_{aux1} and D_{aux3}, and to drain/recover energy from clamp capacitors here is the circuit formed by auxiliary diodes D_{aux2}, D_{aux4}, and auxiliary inductor L_{aux}. Three auxiliary diodes D_{aux2}–D_{aux4} and two auxiliary capacitors C_1 and C_2 are configured in such a way, that: capacitors C_1 and C_2 are connected in series to capture transformer leakage energy when the leakage current inflows into capacitors; the capacitors are connected in parallel to discharge the captured energy.

The behavior of the proposed snubber depends on many snubber parameters. For example, the proposed snubber could work in a resonant mode. The current of the auxiliary inductor resonantly recharges snubber capacitors C_1 and C_2 from one extreme voltage level to another. This increases power losses in the snubber due to higher rms. Also, when the main switch

SW turns OFF, it will take some time for the snubber capacitors to be recharged from the lowest voltage to the voltage when the transformer starts to reverse. This delays the rise of the secondary current. The inductor $L_{\rm aux}$ current can be nonresonant (discontinues or continues) to keep down rms. But if capacitors C_1 and C_2 still have high pulsation then it will result in prolonged transformer reverse time T_x, corresponding adverse consequences like increased rms in flyback, and demand for higher-rated clamp diodes $D_{\rm aux1}$ and $D_{\rm aux3}$. Therefore, the analysis was done for the most efficient version of the proposed snubber: the continuous auxiliary inductor current and the almost constant voltage of clamp capacitors C_1 and C_2.

We will study flyback operation in discontinuous conduction mode (DCM) for generality while snubber inductor $L_{\rm aux}$ current is continuous. The DCM mode is characterized by $T_{\rm on}$ time when the main flyback switch is conducting, $T_{\rm off}$ time when the main switch is turned OFF, and $T_{\rm dis}$–the main transformer discharge time into secondary output. For the flyback topology in steady-state it is well known that $T_{\rm on}$ and $T_{\rm off}$ are related to each other by

$$V_o/_n \times T_{\rm dis} = V_{\rm in} \times T_o \tag{1}$$

where $n = N_s/N_p$ is transformer turns ratio and V_o is the secondary output voltage. Equation (1) is correct for a flyback operating in continuous conduction mode (CCM) also. One could transit to flyback CCM approaching ($T_{\rm off}$–$T_{\rm dis}$) to zero. For analysis we assume: During flyback operation, the sum of two snubber capacitor voltages is higher than the voltage needed to reset a flyback transformer and are constant; all semiconductor switches are ideal. There would be four flyback operation stages to consider. The equivalent circuit diagrams are given in Fig. 3 for each of the four stages. In this analysis, the main attention was paid to the operation of the proposed snubber.

The waveforms in a steady-state condition have been generated in LTspice simulation software for the particular circuit parameters: transformer primary inductance $L_1 = 10\ \mu$H, turns ratio $n = 7$, coupling coefficient between primary and secondary is 0.987 (leakage inductance 0.26 μH), switching frequency is about 69.7 kHz, input voltage $V_{\rm in} = 30$ V, output voltage 205 V, and output power 136 W (output load resistor 310 Ω). The proposed snubber has the parameters: $C_1 = C_2 = 1.5\ \mu$F and $L_{\rm aux} = 2.2$ mH. The duration of the stages and simulated operation waveforms are presented in Fig. 4.

The main switch SW turns ON at the time moment t_0 and the whole switching cycle lasts until the moment t_4. By t_0 auxiliary diodes $D_{\rm aux1}$, $D_{\rm aux3}$, and secondary diode $D_{\rm o}$ are nonconducting.

A. Stage 1 (t_0–t_1)

In this stage, the main switch SW is turned ON, and the transformer starts to gain power. The equivalent schematic of this stage is presented in Fig. 3(a). Auxiliary diode $D_{\rm aux3}$ is reverse biased by the voltage V_c. The auxiliary diode $D_{\rm aux1}$ is reverse biased by the voltage $V_{\rm in} + V_c$. The current I_x of auxiliary inductor $L_{\rm aux}$ increases linearly because two snubber capacitors C_1 and C_2 are applied to the $L_{\rm aux}$ through the main switch SW. The capacitors C_1 and C_2 are connected in parallel through $D_{\rm aux2}$ and $D_{\rm aux4}$ diodes and share the I_x current, see Fig. 4. Let V_c be the steady-state voltage on each of C_1 and C_2, $T_{\rm on} = t_1 - t_0$ then during this stage I_x will increase by value

$$\Delta I_x = V_c/_{L_{\rm aux}} \times T_{\rm on}. \tag{2}$$

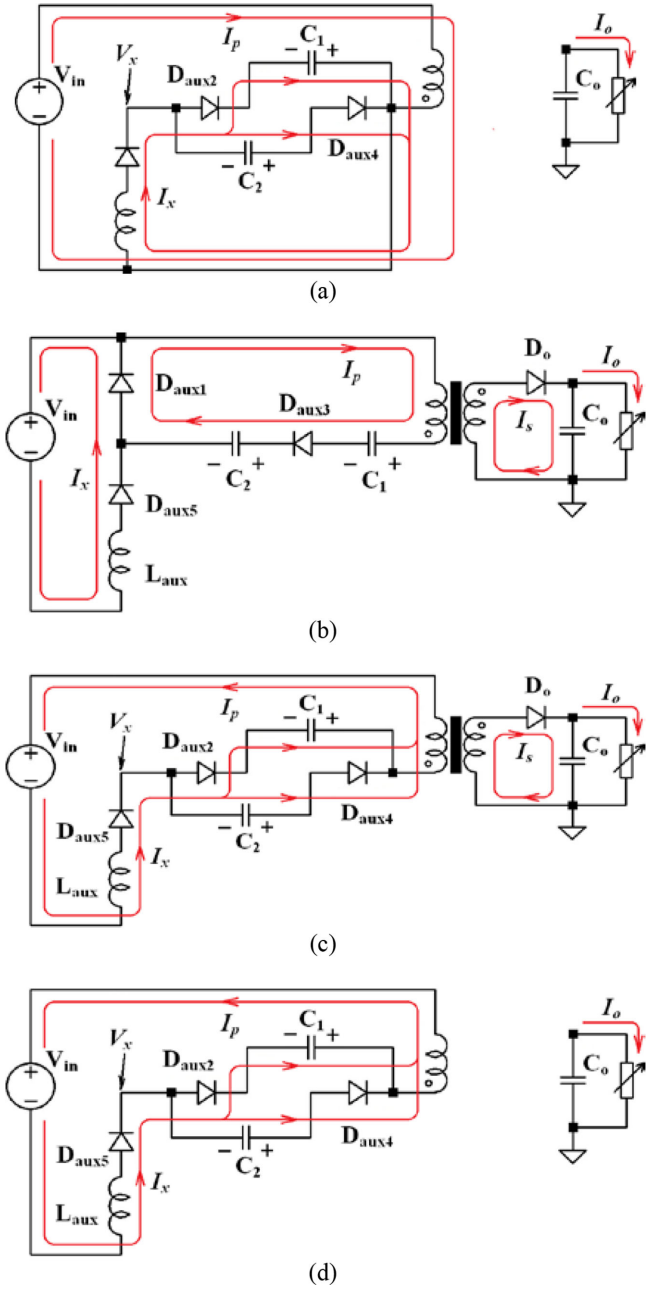

Fig. 3. Equivalent stage circuits. N_p–primary winding turns number, N_s–secondary winding turns number, $V_{\rm in}$–input voltage, I_p–transformer primary current, I_s–transformer secondary current, I_x–auxiliary inductor $L_{\rm aux}$ current, and I_o–output load current. (a) Stage 1. (b) Stage 2. (c) Stage 3. (d) Stage 4.

B. Stage 2 (t_1–t_2)

At the moment, t_1 the main switch SW turns OFF, $I_{\rm SW} = 0$ in Fig. 4, and the transformer primary current I_p is redirected and charges clamp capacitors C_1 and C_2 through the diodes

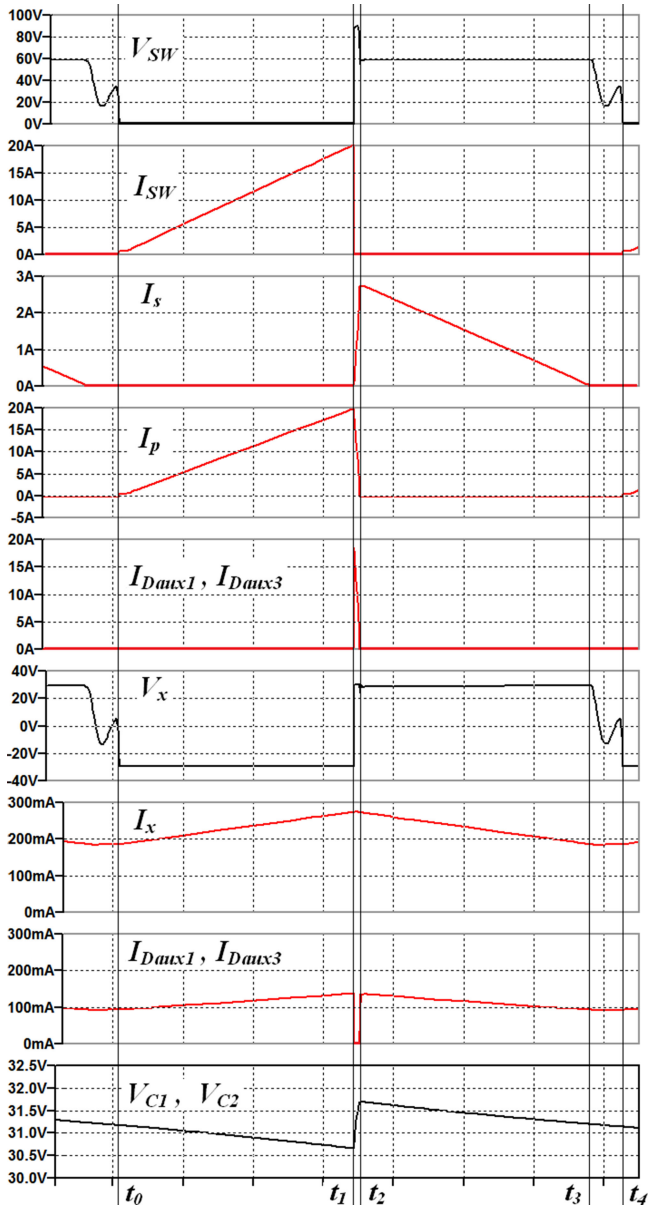

Fig. 4. Simulation waveforms of the flyback converter circuit with the proposed regenerative snubber. $V_{\rm SW}$–drain to source voltage on the switch SW, $I_{\rm SW}$–current of the switch SW, I_s–secondary transformer winding current, I_p–current of the transformer primary, $I_{\rm Daux1}$ and $I_{\rm Daux3}$–currents of corresponding charging diodes $D_{\rm aux1}$ and $D_{\rm aux3}$, V_x–the potential of the $D_{\rm aux5}$ cathode, I_x–current of the auxiliary inductor $L_{\rm aux}$, $I_{\rm Daux2}$, and $I_{\rm Daux4}$ currents of corresponding discharging diodes $D_{\rm aux2}$ and $D_{\rm aux4}$, and V_{C1} and V_{C2}–snubber capacitors C_1 and C_2 voltage values.

$D_{\rm aux1}$ and $D_{\rm aux3}$ until t_2 when transformer leakage energy is depleted. The equivalent schematics of this stage is in Fig. 3(b). The diodes $D_{\rm aux2}$ and $D_{\rm aux4}$ are nonconducting until charging current I_p reverses to $-I_x$ value, by moment t_2. I_x current is redirected to the $D_{\rm aux1}$ and inductor $L_{\rm aux}$ discharges to the input for this short period of time. Auxiliary capacitors C_1 and C_2 connected in series and provide double V_c voltage to reset the main transformer; hence, I_p rapidly reverses

$$\frac{dI_p}{dt} = -\left(2V_c - V_o/n\right) \times 1/L_s \tag{3}$$

where $L_s = L_1 - M^2/L_2$ is the transformer leakage inductance measured from the primary side. L_1, L_2, and M are primary, secondary, and mutual inductances of the transformer, correspondingly. The time duration of this stage T_x can be derived from (3)

$$T_x = t_2 - t_1 = \frac{L_s \times I_{\rm p\_peak}}{2V_c - V_o/n} \tag{4}$$

where $I_{\rm p\_peak}$ is the primary side current peak before transistor SW switch OFF. Deriving (4), snubber inductor current I_x was neglected compared to $I_{\rm p\_peak}$.

C. Stage 3 (t_2–t_3)

The equivalent schematic of this stage is in Fig. 3(c). By the moment t_2, the transformer leakage energy has been depleted, I_p has dropped to $-I_x$ value, and diodes $D_{\rm aux1}$ and $D_{\rm aux3}$ have been closed, $I_{\rm Daux1} = I_{\rm Daux3} = 0$ in Fig. 4. During this time, the transformer secondary side discharges energy into the output capacitor $C_{\rm o}$. The auxiliary inductor current I_x forward biases the diodes $D_{\rm aux2}$ and $D_{\rm aux4}$, and capacitors C_1 and C_2 are connected in parallel. Now, the snubber inductor $L_{\rm aux}$ and capacitors C_1 and C_2 recover part of their energy accumulated in previous stages to the input power supply and into the secondary output through the main transformer. The voltage applied to the $L_{\rm aux}$ equal to $-(V_{in} + V_o/n - V_c)$. Thus, taking into account (1), the I_x current change during discharge time $T_{\rm dis} = {\rm t}_3 - {\rm t}_2$ can be found as

$$\Delta I_x = -\left[V_{\rm in} \times (T_{\rm dis} + T_{\rm on}) - V_c \times T_{\rm dis}\right] \times {}^1/_{L_{\rm aux}}. \tag{5}$$

D. Stage 4 (t_3–t_4)

By the time t_3, the secondary current I_s has exhausted, $I_s = 0$, and the last operation stage starts, see Fig. 3(d). The secondary diode $D_{\rm o}$ is reversed, the main switch $Q_{\rm m}$ remains OFF; therefore, the flyback enters the dwell mode. Now, the energy of the snubber inductor $L_{\rm aux}$ and snubber capacitors C_1 and C_2 are recovered into the input only. The voltage applied to the auxiliary inductor and the transformer primary inductor L_1 is $-(V_{\rm in} - V_c)$. The current I_x will change by value

$$\Delta I_x = -(V_{\rm in} - V_c) \times {}^{T_{\rm dw}}/_{(L_{\rm aux} + L_1)} \tag{6}$$

where dwelling time $T_{\rm dw} = t_4 - t_3$ or $= T_{\rm off} - T_{\rm dis}$.

III. Discussion

In steady-state the auxiliary inductance current does not change during flyback switching cycle $\Delta I_x = 0$.

Therefore, combining changes (2), (5), and (6) of ΔI_x for stages 1, 3, and 4, and neglecting the change (3) of I_x during stage 2, one could find that

$$V_c \times T_{\rm on} - V_{\rm in} \times (T_{\rm dis} + T_{\rm on}) + V_c \times T_{\rm dis} - (V_{\rm in} - V_c) \times T_{\rm dw} \times {}^{L_{\rm aux}}/_{(L_{\rm aux} + L_1)} = 0 \tag{7}$$

from which it is easily found that

$$V_c = V_{\rm in} \tag{8}$$

which means, the voltages of auxiliary snubber capacitors C_1 and C_2 in Fig. 2 follow input voltage. At stage 2, the transformer primary current I_p is met by resetting double input voltage $2V_{\rm in}$ of serially connected snubber capacitors. Equation (8) was derived assuming that the auxiliary inductor current is continuous. It can be said that the auxiliary inductance recovers energy to the secondary side at stage 3 through the flyback transformer.

In most practical cases, the conventional LCD snubber in Fig. 1 is implemented with a resonant current of the auxiliary inductor $L_{\rm x}$ and recharging snubber capacitor $C_{\rm x}$ [10]–[12]. The snubber can also be implemented with a nonresonant (discontinuous or continuous) auxiliary inductor current. In some rare cases, the snubber could be implemented with constant voltage V_c of the capacitor C_x. In this case, with continuous conducting inductor $L_{\rm x}$, the steady-state equations for the $L_{\rm x}$ current would be the same as at stages 1, 3, and 4 of the proposed snubber, and hence we get the same steady-state value for $V_c = V_{\rm in}$, like in the case of the proposed snubber (8). The advantages for the conventional LCD snubber operating in the nonresonant mode before the resonant mode are as follows:

1) the auxiliary inductance $L_{\rm x}$ recovers energy to the secondary side;
2) snubber capacitor $C_{\rm x}$ does not recharge;
3) no delay of the secondary current;
4) reduced circulating currents in the snubber and flyback.

The conventional snubber will work in this mode correctly if clamp voltage V_c is big enough to reverse the transformer at a reasonable time T_x, therefore $V_c = V_{\rm in} > V_o/n$. For the flyback working in CCM, it means that duty cycle $D < 50\%$. It is a too tight limitation, which is why the conventional LCD snubber is never designed with constant V_c voltage. At least, the snubber capacitor is designed to charge and discharge with sufficient voltage swings around the $V_{\rm in}$ value. This poses the trade-off problem between the voltage spike of the main switch and the delay time T_x. As for the proposed snubber in Fig. 2, the considered mode of operation will be valid for the clamp voltage $2V_c$

$$2V_c > V_o/n. \tag{9}$$

For example, for continuous conducting flyback, (9) means the duty cycle $D < 2/3$. Most of the flyback designs can fit the limit (9). The advantage is that, at the transformer reverse stage 2, the reverse voltage is $2V_{\rm in}$. Therefore, with the proposed snubber, the flyback has reduced reverse time T_x, decreased power losses in the power train due to reduced rms, and less power handled by the snubber. If double clamping voltage $2V_{\rm in}$ is an undesirable voltage stress for the primary flyback switch, designers could reduce clamping voltage according to (12).

Let us cover the case when the auxiliary inductor current I_x is discontinuous, C_1 and C_2 voltages are constant.

1) To be specific, let the current I_x vanish somewhere at stage 4, when the flyback is at the dwell mode. The current I_x will change by value

$$\Delta I_x = -(V_{\rm in} - V_c) \times T_y \times {}^{L_{\rm aux}}\!/_{(L_{\rm aux} + L_1)} \tag{10}$$

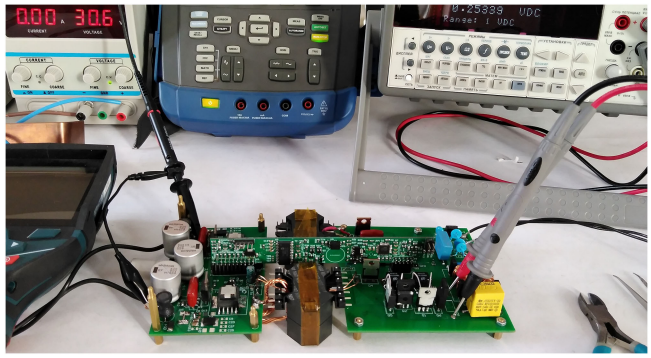

Fig. 5. Photo of the experimental setup of the microinverter with two-phased flybacks.

where T_y is the I_x current time tail to extinct at stage 4. By assumption $T_y < T_{\rm dw}$. Combining changes (2), (5), and (10) of ΔI_x one could come to the same result (8).

2) To be specific, let the current I_x reach zero somewhere at stage 3, when the flyback is at the discharge mode. The auxiliary inductor $L_{{\rm aux}x}$ current will change by value

$$\Delta I_x = -(V_{\rm in} + V_o/n - V_c) \times {}^{T_z}\!/_{L_{\rm aux}} \tag{11}$$

where T_z is the I_x tail to extinct at stage 3. By assumption, $T_z < T_{dis}$. Combining changes (2) and (11) of ΔI_x, one can get

$$V_c = (V_{\rm in} + V_o/n) \times {}^{Tz}\!/_{(T{\rm on} + Tz)}. \tag{12}$$

This means with decreasing T_z, the V_c goes down. The adverse effect of discontinuous conduction is that if V_c decreases, then this results in prolonged reverse time T_x and, as a consequence, higher rms in the flyback.

The charge Q_x pumped into clamp capacitors C_1 and C_2 during transformer reverse time T_x can be estimated as

$$Q_x = \frac{1}{2} I_{\rm p\_peak} \times T_x \tag{13}$$

where the 1/2 multiplier comes up because the current I_x linearly decreases to zero during T_x. The auxiliary inductance current I_x must discharge the clamp capacitors during the switching period $T_{\rm sw}$; hence, from (13) one could find the average current I_x

$$\langle I_x \rangle = \frac{E_x}{V_c \times T_{\rm sw}} \text{ or } \langle I_x \rangle = \frac{1}{T_{\rm sw}} \frac{L_s \times I_{\rm p\_peak}^2}{2V_c - V_o/n} \tag{14}$$

where E_x is the part of the leakage energy captured by clamp capacitors C_1 and C_2.

The above equations and conclusions are obtained for flyback in DCM, but the same result is correct for a flyback in CCM.

IV. Experimental Results

A laboratory sample has been created, see Fig. 5, to verify theoretical conclusions in experiments.

The experimental flyback sample has the switching frequency 69.7 kHz, and the transformer with measured parameters is presented in Table I.

With these parameters, the converter operates in CCM over an input power range of 100 to 300 W. The idea behind the transformer design was to reduce rms currents with attention to

TABLE I
FLYBACK TRANSFORMER PARAMETERS

Core	Material	Turns ratio	Primary inductance	Secondary inductance	Leakage, primary	Leakage, secondary
PQ4040	PC97	10/80	31.4uH	2.01mH	0.45uH	46.3uH

TABLE II
PARAMETERS OF THE SNUBBERS

Conventional LCD (Fig. 2)	D_1: 150V, 5A, SMC	C_x= 8x15nF, case 8x1206	L_x=2.2mH, 0.7A, 2.2Ohm, size=12x16mm	D_2: 150V, 2A, SMA case
The proposed (Fig. 4)	D_{aux1}, D_{aux3}: 150V, 5A, SMC	C_1=C_2= 6x0.2uF, case 6x1206	L_{aux}=2.2mH, 0.7A, 2.2Ohm, size=12x16mm	D_{aux2}, D_{aux4}: 150V, 2A, SMA

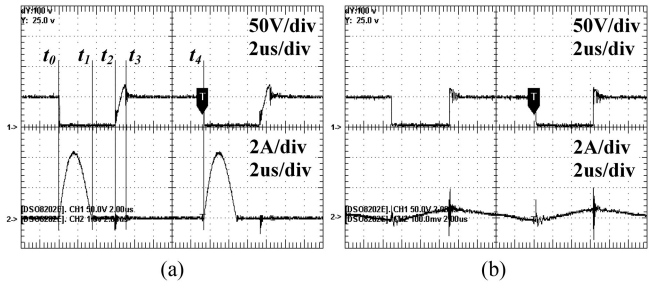

Fig. 6. Conventional snubber, top—drain–source voltage of the main switch (Q_m or SW), lower—the current I_x of auxiliary L_x. (a) Resonant I_x. (b) Continuous I_x.

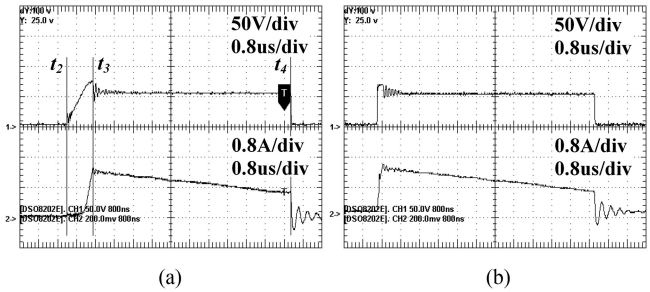

Fig. 7. Conventional snubber, top—drain-source voltage of the main switch (Q_m or SW), lower—the secondary side current I_s. (a) Resonant I_x. (b) Continuous I_x.

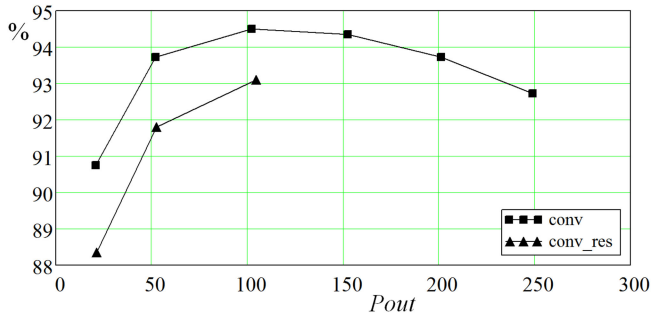

Fig. 8. Efficiency: conv—conventional LCD snubber with continuous I_x; conv_res—conventional LCD snubber with resonant I_x.

the primary side because it is a high current part of the flyback circuit. Pursuing our ultimate goal, we moved from boundary conduction mode to CCM by increasing transformer primary inductance. By decreasing the transformer turns ratio ($n = 1/8$), the conduction time of the main switch was increased, so the duty cycle values are around 50% at maximum power. Increasing magnetizing inductance also increases the leakage inductance, but if we designed the snubber with perfect recovery efficiency, then leakage inductance issues might not be critical. Also, we had in our mind that reducing the peak of the primary current would make the leakage energy problem not that problematic for the proposed snubber.

The conventional LCD snubber and the proposed snubber have parameters presented in Table II. The capacitors of the snubbers are made of parallel-connected capacitors to reduce equivalent series resistance (ESR) and power losses.

A. Conventional Snubber

First, we compared the performances of the conventional snubber (Fig. 1) with resonant and continuous conducting auxiliary inductances. The waveforms were measured for the flyback in CCM at input voltage 35 V, output voltage 180 V, and output power 100 W.

In Figs. 6(a) and 7(a), one can see the experimental waveforms with resonant auxiliary L_x. The snubber parameters are almost the same as in Table II, except for the $L_x = 8.6\ \mu$H, 10 A (size 10x25 mm, $Rx = 60\ \text{m}\Omega$). During time interval t_0–t_1, the snubber capacitor C_x is resonantly recharged to the lowest voltage. During time interval t_2–t_3, the snubber capacitor is linearly recharged back to the highest voltage by the primary current while the flyback transformer reverses. This reverse process takes considerable time T_x more than 0.8 μs, see the delay of the secondary side current in Fig. 7(a). The charge flowing into the C_x capacitor could be estimated as $Q_x = T_x \times I_{s\_peak}/n = 0.8\ \mu\text{s} \times 1.25\ \text{A} \times 8 = 8\ \mu\text{Q}$.

In Figs. 6(b) and 7(b), one can see the experimental waveforms for the conventional LCD snubber with a continuous conducting current of L_x. The snubber parameters are the same as in Table II. The inductor L_x current is slightly above CCM, capacitor C_x does not recharge. As a consequence of continuous conduction, the L_x damps energy into the secondary side, and there is no C_x recharge, and no much delay T_x between the switch Q_m turn-OFF and the secondary side current [see Fig. 7(b)]. Therefore, there are considerably lower power losses in the snubber circuit and there is no adverse influence on flyback rms. Notice that the voltage of the snubber capacitor is constant, the voltage spike on main switch $2V_{in} = 70$ V.

In Fig. 8, one can compare the flyback efficiencies with the conventional nonintegrated LCD snubber with resonant and continuous conducting auxiliary inductance L_x.

The measurements with the resonant L_x cannot be continued above the 120 W flyback output because of the considerable heating of the capacitor C_x array. It appears that the conduction losses are predominant. The efficiency of the hard switching flyback with a nonresonant conventional LCD snubber is considerably higher than the soft switching flyback with the same resonant snubber.

In Figs. 9(a) and 10(a), there are experimental waveforms of the flyback at 260 W output power, 280 V output voltage, and the

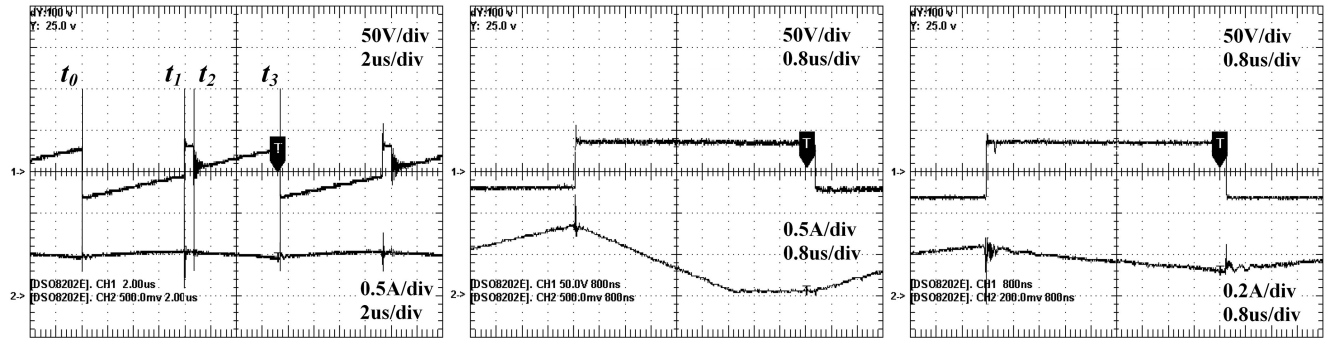

Fig. 9. Snubbers comparison, top waveform–potential of clamp diode (D_1 or D_{aux1}) anode, lower waveform–auxiliary inductor current I_x. (a) Conventional LCD snubber, continuous I_x. (b) Proposed snubber, discontinuous I_x. (c) Proposed snubber, continuous I_x.

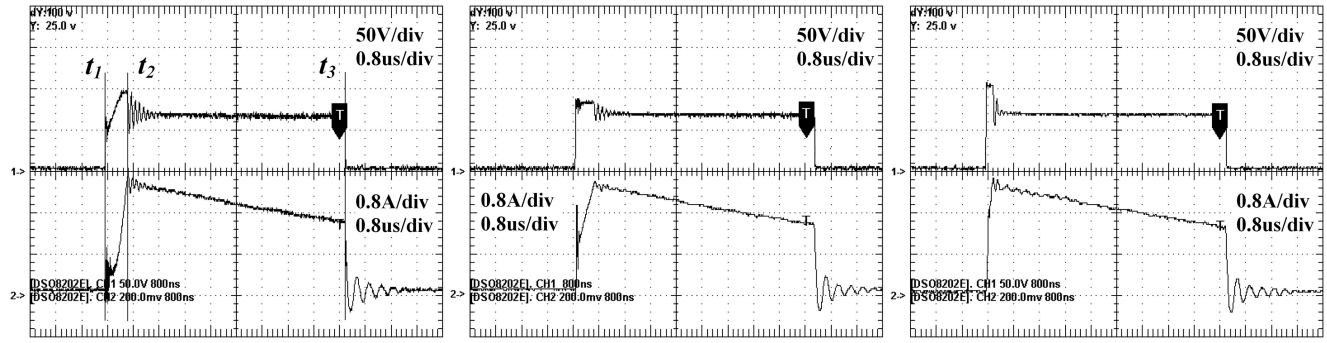

Fig. 10. Snubbers comparison, top waveform–the drain-source voltage of the main switch ($\mathrm{Q_m}$ or SW), lower waveform–the secondary side current I_s. (a) conventional LCD snubber, continuous I_x. (b) Proposed snubber, discontinuous I_x. (c) Proposed snubber, continuous I_x.

continuous conducting auxiliary inductance of the conventional snubber. The test experiments were done at input voltage 35 V. It is seen that the clamp voltage starts to swing with considerable amplitude because its steady-state value $V_c = V_{in}$ is no longer capable to reverse the transformer. By the moment t_1 transistor $\mathrm{Q_m}$ turns OFF and during t_1–t_2 capacitor C_{x} almost linearly charged to the maximum about 52 V. During this transformer reverse time $T_x = t_2 - t_1$, clamp capacitor recycles to the input the rest of the leakage energy and captures a new portion of it. Because some leakage energy is recovered during t_2–t_3 to the secondary side, it takes less time to recover the rest of leakage during t_1–t_2 of the next switching cycle; therefore, $T_x = t_2 - t_1$ is shorter than in the case of resonant L_{x}. Notice that at 260 W output, T_x is 0.5 μs [see Fig. 9(a)] and compare it to reverse time 0.8 μs in Fig. 7(a) for the 100 W case with resonant L_{x}. The charge flowing into C_{x} during T_x: $Q_x = T_x \times I_{\mathrm{s\_peak}}/n$ = 0.5 μs $\times$ 2.28 A $\times$ 8 = 8.7 μQ–practically the same as with the resonant L_x and 100 W output power, but snubber rms is considerably lower due to the continuous nature of I_x. The thermal measurements give that the C_x capacitor array heats over 110 °C at 100 W flyback power with resonant I_x and heats up to 80 °C at 260 W with the continuous current I_x.

B. Proposed Snubber

In Figs. 9 and 10, there are waveforms of the flyback with the implemented proposed snubber. The measurements were done at the flyback output power 250 W, output voltage 280 V, and input 35 V. Figs 9(b) and 10(b) are for the auxiliary L_{aux} discontinuous current with snubber parameters are almost the same as in Table II except for the auxiliary inductance $L_{\mathrm{aux}} =$ 100 μH, 2.2 A (size 10x20 mm, $R_{\mathrm{aux}} = 90$ mΩ). Figs 9(c) and 10(c) are for the L_{aux} continuous current with snubber parameters are as in Table II.

With the continuous current of the snubber inductor L_{x}, as shown in Fig. 10(c), the voltage spike on the flyback switch is about $3V_{\mathrm{in}} = 105$ V and in coincidence with (8). With the discontinuous current of L_{x}, Fig. 10(b), the voltage spike on the flyback switch is noticeably lower than $3V_{\mathrm{in}}$ according to (12). Therefore, the transformer reverse time $T_x = 0.6$ μs is considerably longer than in the case of the continuous conducting L_{x}, compare to $T_x = 0.25$ μs in Fig. 10(c). This results in higher rms currents in the flyback circuit and the snubber. In Fig. 11, one can compare efficiencies of the proposed snubber with continuous and discontinuous I_x current. As it was expected, the efficiency of the flyback with discontinuous I_x is lower than the efficiency with continuous I_x.

C. Comparison of the Snubbers

Comparing Fig. 10(a) with (c), one can see that the transformer reverse time T_x is considerably shorter with the proposed snubber than with the conventional LCD snubber. Therefore, higher flyback efficiency is expected because of smaller rms.

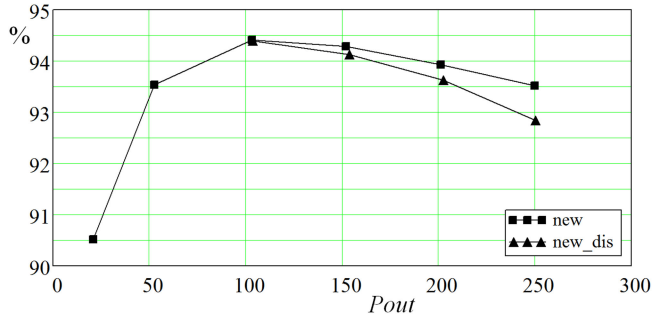

Fig. 11. Efficiency: new–the proposed snubber with continuous I_x, new_dis–the proposed snubber with discontinuous I_x.

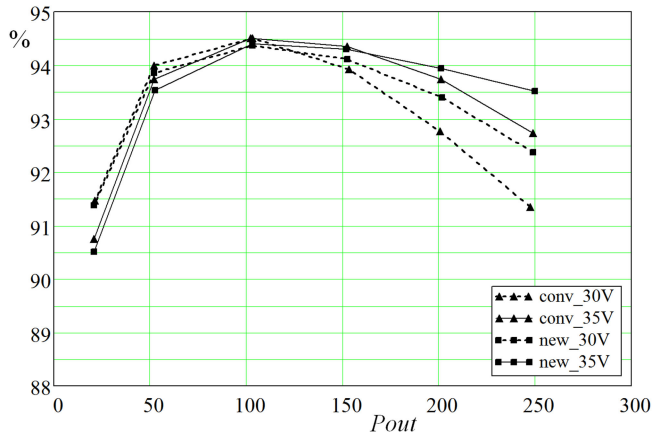

Fig. 12. Efficiency measurements, constant resistive load 310 Ω: triangle–conventional LCD snubber, square–the proposed snubber; dotted–30 V input, solid–35 V input.

TABLE III
280 V CONSTANT VOLTAGE LOAD, $P_{\rm OUT} = 262$ W

Vin, V	$V_{SW\ peak}$, V	I_x, A	$I_{s\ peak}$	$I_{s\ RMS}$	$I_{p\ peak}$	Snubber
35V	104	0.16	2.16A	1.29A	18.0A	New
	98	0.46	2.25A	1.35A	18.9A	Conven.
30V	91	0.52	2.19A	1.32A	19.7A	New
	102	0.65	2.35A	1.38A	21.4A	Conven.

The conventional snubber has a bigger auxiliary inductance current of about 0.5 A [see Fig. 9(a)] while the proposed one has below 0.2 A. This is because during prolonged time T_x, the conventional snubber clamps more charge and that charge needs to be recovered by increased auxiliary inductor current.

Finally, the flyback efficiencies with the conventional LCD and the proposed snubbers were measured at their best performance conditions with continuous conduction currents in auxiliary inductances (Figs. 12 and 13).

The measurements were provided at two input voltages 30/35 V and two loads: constant resistive load 310 Ω (Fig. 12) and constant output voltage 280 V (Fig. 13). The value of the capacitor C_x of the conventional snubber was chosen to have about the same maximum voltage spike about 104 V on the flyback primary switch over input voltage and output load ranges as with the proposed snubber, see Table III. The transformer reverse time T_x increases with load faster for the conventional snubber than for the proposed one. Therefore, at loads more than 100 W, the efficiency of the proposed snubber is better.

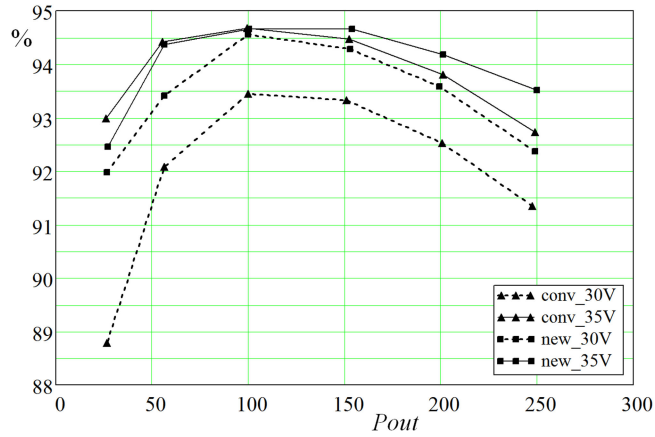

Fig. 13. Efficiency measurements, constant output voltage 280 V: triangle–conventional LCD snubber, square–the proposed snubber; dotted–30 V input, solid–35 V input.

TABLE IV
CONVENTIONAL SNUBBER POWER LOSS BREAKDOWN

Component	Parameter	Current	Formula	Power loss
Inductor L_x	R_x=2.2 Ω	I_x=0.46A	$R_x*I_x^2$	0.47W
Diode D_2	V_{D2}=0.3V	I_x=0.46A	$V_{D2}*I_x$	0.14W
Diode D_1	V_{D1}=0.4V	I_{D1}=0.79A	$V_{D1}*I_{D1}$	0.32W
Capacitor C_x	ESR=0.02 Ω	I_c=3.86A	ESR*(I_c^2+I_x^2)	0.3W+0.0W
Total for the conventional LCD snubber:			Σ power loss	=1.23W
Efficiency loss			Σ/Pin	0.46%

At output loads lower than 100 W, the T_x time of both flybacks becomes negligible to adversely influence flyback rms. The leakage energy drops and the auxiliary inductance current I_x becomes discontinuous in the proposed snubber, switching losses of the snubber diodes $D_{\rm aux2}$ and $D_{\rm aux4}$ become dominant. Therefore, at loads $\leq$100 W and D $<$ 50%, the efficiency of the proposed snubber is slightly worse than the efficiency of the conventional snubber. At input voltage 30 V and constant output 280 V, the efficiency of the conventional snubber is considerably worse over the entire load range. This is because at the given input and output voltages the flyback duty cycle is close to 50% over the entire load range; therefore, increased currents circulate in the snubber considerably recharging the capacitor C_x and waste more power in the snubber circuit.

From Table III, the peak primary current, peak secondary current, and secondary rms have about 5% gain over the proposed snubber case at the maximum output power 250 W. It can be said with confidence that the primary rms is affected the same way, though not directly measured because of high sensitivity to intrusions to the primary side.

Let us evaluate snubber losses at input voltage 35 V, output voltage 280 V, and output power 262 W. The component losses of the conventional snubber are listed in Table IV. The average current of the diode D_1 was estimated as peak current $I_{\rm p\_peak} = 18.9$ A of the primary switch $Q_{\rm m}$ multiplied by the fraction of the transformer reverse time $\Delta T_x = 0.6$ μs [estimated from Fig. 10(a), $T_x = 0.8$ μs] and divided by the switching period $T_{\rm sw} = 14.4$ μs

$$I_{D1} = I_{\rm p\_peak} \times {}^{\Delta T_x}/_{T_{\rm sw}}. \tag{15}$$

TABLE V
PROPOSED SNUBBER POWER LOSS BREAKDOWN

Component	Parameter	Current	Formula	Power loss
Inductor L_{aux}	R_x=2.2 Ω	I_{aux}=0.16A	$R_x*I_{aux}^2$	0.06W
D_{aux2}, D_{aux4}, D_{aux5}	V_{D2}=0.3V	I_{aux}=0.16A	$2V_{D2}*I_{aux}$	0.10W
D_{aux1}, D_{aux3}	V_{D1}=0.4V	I_{D1}=0.16A	$2V_{D1}*I_{D1}$	0.13W
Capacitors C_1, C_2	ESR=0.02Ω	I_c=1.7A	$2ESR(I_c^2+I_x^2)$	0.06W
Total for the proposed snubber:			Σ power loss	0.35W
Efficiency loss			Σ/Pin	0.13%

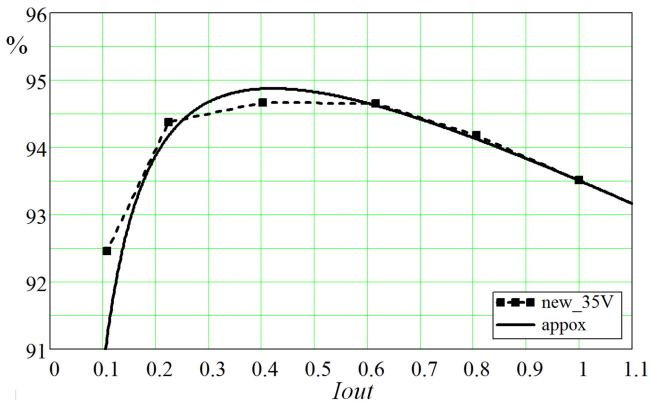

Fig. 14. Approximation of the efficiency data.

The rms current of the snubber capacitor C_x was estimated as

$$I_c = \sqrt{I_{\text{p\_peak}}{}^2 \times {\Delta T_x}/{T_{\text{sw}}}}. \tag{16}$$

The component losses of the proposed snubber are listed in Table V. The average current of the diodes D_{aux1} and D_{aux3} was estimated as peak current $I_{\text{p\_peak}} = 18.0$ A of the primary switch SW multiplied by the transformer reverse time $T_x = 0.25$ μs, divided by the switching period $T_{\text{sw}} = 14.4$ μs and divided by two because the diodes current drops linearly during T_x

$$I_{D1} = \frac{1}{2} I_{\text{p\_peak}} \times {\Delta T_x}/{T_{\text{sw}}}. \tag{17}$$

The rms current of the snubber capacitors C_1 and C_2 was estimated as

$$I_c = \frac{1}{2}\sqrt{I_{\text{p\_peak}}{}^2 \times {\Delta T_x}/{T_{\text{sw}}}}. \tag{18}$$

The conventional snubber accounts for the additional efficiency loss of about 0.33% at 250 W output power.

The flyback power losses comprise switching losses that are linearly dependent on currents and conduction losses that are dependent on square rms. To correctly estimate the influence of the increased rms of the flyback currents, we should estimate the weight of the switching and conduction losses. We approximated the efficiency curve measured at 35 V input and constant output voltage 280 V by the formula

$$\text{Eff} = 100\% - {0.80}/{I_{\text{out}}} - 1.48 - 4.23 \times I_{\text{out}} \tag{19}$$

where I_{out} is output current expressed in dimensionless units referred to the maximum output current. The quality of the approximation can be viewed in Fig. 14. In (19), the subtracted term 1.48 corresponds to the switching losses and the subtracted term $4.23 \times I_{\text{out}}$ corresponds to the conduction losses. The weights of each term at the maximum output power are $W_{\text{sw}} = 1.48\%$ and $W_{\text{con}} = 4.23\%$, here $I_{\text{out}} = 1$. From Table III, the secondary rms of the conventional snubber $I_{\text{s\_RMS}} = 1.35$ A is about 4.7% higher than the secondary $I_{\text{s\_RMS}} = 1.29$ A with the proposed snubber. Assuming that the primary rms is affected by the same amount, one can get influence on the efficiency as

$$\Delta\text{Eff} = W_{\text{sw}} \times 0.047 + W_{\text{con}} \times 0.047^2 = 0.48\%. \tag{20}$$

Hence, the estimation of the efficiency drop is about 0.8% and explains the measurement results in Figs. 12 and 13 at 35 V input and maximum power.

The additional components of the proposed snubber take a little space on the printed circuit board (PCB) (see Table II). Comparing Tables IV and V, it is clear that the proposed snubber could be optimized further: current ratings of diodes D_{aux1} and D_{aux3} could be reduced two times compared to the conventional snubber; ratings of D_{aux2}, D_{aux4}, and D_{aux5} could be reduced to 1 A; thermal ratings of all snubber components could be reduced.

The snubber diode D_{aux5} is helpful in case of high current pulsations in auxiliary inductance L_{aux} and prevents negative current if L_{aux} enters into DCM. If the operation condition (9) of the proposed snubber is valid then the diode D_{aux5} can be removed, because diodes D_{aux2} and D_{aux4} will prevent L_{aux} from negative currents while the diode D_{aux3} will be reverse biased by snubber capacitors C_1 and C_2.

Although we have got the efficiency gain for load >50%, it is possible to extend the achievement down to 25% load in a two-phased converter by smart control. For example, at 25–50% load of the microinverter, one of its phases can be turned OFF to let the other phase operate at 50–100% of its power with the highest efficiency.

The voltage stress on the main switch can be adjusted by introducing the snubber into DCM (12). Practically in all designs, the conventional LCD snubber (resonant or nonresonant) imposes a delay of the flyback secondary side current [Fig. 8(a)]. This is because it takes some time for the clamp capacitor to reach the value sufficient to reverse the flyback transformer. Therefore, given the same voltage stress, the proposed snubber, although in discontinues mode, has advantages.

The proposed snubber suggests more possibilities to study. In the proposed snubber, an integration of a snubber auxiliary inductor with the main flyback transformer is possible. It can be resonant as well if the application requires it. It could be implemented with one or two snubber capacitors resonantly recharging.

V. CONCLUSION

The new passive lossless snubber is proposed in the article. For the proposed snubber, the best operation mode is considered, which better suits microinverter applications or in general, for applications where conduction losses prevail over switching losses. In this article, it was revealed how the conventional LCD snubber adversely influences the flyback efficiency. For low voltage applications such as a microinverter for photovoltaic

panels, a method has been proposed to improve the performance of a conventional snubber. In this particular case, switching losses are small and ZVS can be ignored. It has been shown that the traditional snubber will perform better with the constant voltage of the snubber capacitor although the primary switch is left hard switching. The method is limited to the duty cycles <50%. Therefore, in this article, the improvement for the conventional LCD snubber was proposed. The benefits of the proposed nonresonant snubber are reduced circulating currents in snubber circuits and the snubber does not worsen current rms on flyback primary and secondary sides. Experimental proofs and power loss calculations are provided. The improvement is inexpensive and does not require a lot of space on the PCB.

REFERENCES

[1] T. F. Wu, S. A. Liang, and C. H. Lee, "A family of isolated single-stage ZVS-PWM active-clamping converters," in *Proc. IEEE PESC*, vol. 2, 1999, pp. 665–670.

[2] Q. Li and F. C. Lee, "Design consideration of the active-clamp forward converter with current mode control during large-signal transient," in *Proc. IEEE PESC*, vol. 2, 2000, pp. 966–972.

[3] R. Watson, F. C. Lee, and G. C. Hua, "Utilization of an active-clamp circuit to achieve soft switching in flyback converters," *IEEE Trans. Power Electron.*, vol. 11, no. 1, pp. 162–169, Jan.1996.

[4] T.-F. Wu, Y.-S. Lai, J.-C. Hung, and Y.-M. Chen, "An improved boost converter with coupled inductors and buck-boost type of active clamp," in *Proc. Ind. Appl. Conf.*, 2005, pp. 639–644.

[5] S.-Y. Tseng, C.-.T. Hsieh, and H.-C. Lin, "Active clamp interleaved flyback converter with single-capacitor turn-off snubber for stunning poultry applications," in *Proc.IEEE Power Electron. Drive Syst. Conf.*, 2007, pp. 1401–1408.

[6] M. Fornage, "Method and apparatus for a leakage energy recovery circuit," U.S. Patent US2009/0225574A1, Sep. 10, 2009.

[7] G. A. Kern and T. Gopalarathnam, "Power converter and methods for active leakage energy recovery in a power converter," U.S. Patent US2013/0343098A1, Dec. 26, 2013.

[8] G. Balbayev, A. Nussibaliyeva, B. Tultaev, E. Dzhunusbekov, G. Yestemessova, and A. Yelemanova, "A novel regenerative snubber circuit for flyback topology converters," *J. Vibroengineering*, vol. 22, no. 4, pp. 983–991, Jun. 2020.

[9] T. Ninomiya, T. Tanaka, and K. Harada, "Analysis and optimization of a nondissipative LC turn-off snubber," *IEEE Trans. Power Electron.*, vol. 3, no. 2, pp. 1147–1156, Apr. 1988.

[10] R. Petkov and L. Hobson, "Analysis and optimization of a flyback convertor with a nondissipative snubber," *IEE Proc. Electric Power Appl.*, vol. 142, no. 1, pp. 35–42, Jan. 1995.

[11] M. Hirokawa and T. Ninomiya, "Nondissipative snubber for rectifying diodes applied to a front-end power supply," in *Proc. IEEE PCC-Osaka*, vol. 3, 2002, pp. 1176–1181.

[12] C. Liao and K. Smedley, "Design of high efficiency flyback converter with energy regenerative snubber," in *Proc. IEEE App. Power Electron. Conf. Expo.*, TX, USA, 2008, pp. 796–800.

[13] J. Qian and D. F. Weng, "Leakage energy recovering system and method for flyback converter," U.S. Patent US 6473318, Oct. 29, 2002.

[14] A. Abramovitz, "Analysis and design of energy regenerative snubber for transformer isolated converters," *IEEE Trans. Power Electron.*, vol. 29, no. 11, pp. 6030–6040, Nov. 2014.

[15] Q. Jinrong and F. Weng Da, "Voltage clamping system and method for a dc/dc converter," U.S. Patent WO02/41479A2. May 23, 2002.

[16] T.-H. Ai, "A novel integrated nondissipative snubber for flyback converter," in *Proc. IEEE Int. Conf. Syst. Signals*, Jun. 2005, pp. 66–71.

[17] M. Mohammadi and M. Ordonez, "Flyback lossless passive snubber," in *Proc. IEEE Energy Convers. Congr. Expo.*, 2015, pp. 5896–5901.

[18] E. J. Dzhunusbekov and S. A. Orazbayev, "Switch mode power converter apparatus and method for a transformer leakage energy recovery," Eurasian Patent EAPO№035584B1, Jul. 14, 2020.

Erlan Dzhunusbekov received the Ms.D. degree in solid-state physics from the Russian National Research Nuclear University (MEPhI), Moscow, Russia, in 1996.

He has been the Lead Engineer with the R&D Forward-Looking Group of Power Electronics in the Russian National Research University (MAI), Moscow, Russia. He has been the Principal Engineer with the Power Advanced Team, Samsung Electro-Mechanics Company, Gyeonggi-do, South Korea. Currently, he is the Principal Investigator with the Electronics Laboratory of Advanced R&D, Kazakh-British Technical University, Almaty, Kazakhstan.

Sagi Orazbayev received the Ph.D. degree in the field of materials science and technology of new materials from Al-Farabi Kazakh National University, Almaty, Kazakhstan, in 2015.

He is a Postdoctoral Researcher with the Al-Farabi Kazakh National University, where he is also a Senior Researcher with the National Nanotechnology Laboratory. His research interests include the general areas of plasma processing science and gas discharge phenomena, especially as applied to nanotechnology applications, light sources, solar energy utilization, and power electronics. He studies the physics and chemistry of chemically active nonequilibrium plasmas, related to dust particle nucleation and growth indifferent kinds of chemistries and different applications. He and his group work closely with various plasma users for material processing and the production of diagnostic equipment.